Cell, Vol. 123, 119–132, October 7, 2005, Copyright ©2005 by Elsevier Inc. DOI 10.1016/j.cell.2005.08.001

The Rho/Rac-Family Guanine Nucleotide Exchange Factor VAV-1 Regulates Rhythmic Behaviors in *C. elegans*

Kenneth R. Norman,[1,5] Robert T. Fazzio,[1,2,5] Jerry E. Mellem,[1] Maria V. Espelt,[4] Kevin Strange,[4] Mary C. Beckerle,[1,2] and Andres V. Maricq[1,3,*]
[1]Department of Biology
[2]Huntsman Cancer Institute
[3]The Brain Institute
University of Utah
Salt Lake City, Utah 84112
[4]Department of Anesthesiology
Vanderbilt University Medical Center
Nashville, Tennessee 37232

Summary

Rhythmic behaviors are a fundamental feature of all organisms. Pharyngeal pumping, the defecation cycle, and gonadal-sheath-cell contractions are three well-characterized rhythmic behaviors in the nematode *C. elegans*. The periodicities of the rhythms range from subsecond (pharynx) to seconds (gonadal sheath) to minutes (defecation). However, the molecular mechanisms underlying these rhythmic behaviors are not well understood. Here, we show that the *C. elegans* Rho/Rac-family guanine nucleotide exchange factor, VAV-1, which is homologous to the mammalian Vav proto-oncogene, has a crucial role in all three behaviors. *vav-1* mutants die as larvae because VAV-1 function is required in the pharynx for synchronous contraction of the musculature. In addition, ovulation and the defecation cycle are abnormal and arrhythmic. We show that Rho/Rac-family GTPases and the signaling molecule inositol triphosphate (IP_3) act downstream of VAV-1 signaling and that the VAV-1 pathway modulates rhythmic behaviors by dynamically regulating the concentration of intracellular Ca^{2+}.

Introduction

Rhythmic activities are ubiquitous biological phenomena and can be observed in cells, tissues, and the behavior of most organisms. Biological rhythms regulate many diverse processes, such as heartbeat, breathing, locomotion, and gut peristalsis. The molecular machinery underlying the generation and regulation of rhythms less than a day in duration—known as ultradian rhythms—are not well understood. To gain a molecularly based understanding of these biological rhythms, the use of a genetically tractable organism has certain advantages. *C. elegans* hermaphrodites have three well-characterized rhythmic behaviors. These include pharyngeal peristalsis that occurs every 1–2 s (Avery and Thomas, 1997), gonadal-sheath-cell contractions that occur every 7 s (McCarter et al., 1997), and the defecation motor program that occurs approximately every 45–50 s (Thomas, 1990). Interestingly, these rhythms are considered nonneurogenic because they can still be observed following perturbation of nervous-system function. Some of these rhythmic behaviors appear to be regulated by changes in intracellular Ca^{2+} concentration (Dal Santo et al., 1999; Lee et al., 1997).

One candidate molecule that is hypothesized to link activation of receptors at the cell surface to the initiation and control of Ca^{2+} oscillations is the proto-oncogene Vav1, which along with other Vav family members has a key role in regulating Ca^{2+} signaling in hematopoietic cells (Bustelo, 2001; Turner and Billadeau, 2002). Interestingly, Vav2 and Vav3 are expressed in many other tissues, including the nervous system and cardiac muscle, where their function is not well understood (Movilla and Bustelo, 1999; Schuebel et al., 1996). Vav proteins contain multiple functional domains, including a Src homology 2 (SH2) domain that links upstream signaling events to Vav activation and a Dbl homology (DH) domain that functions as a guanine nucleotide exchange factor (GEF) in the activation of downstream Rho/Rac GTPases (Bustelo, 2001; Turner and Billadeau, 2002). Following stimulation of the T cell antigen receptor (TCR), Vav1 is phosphorylated, which turns on GEF function and leads to the activation of Rho/Rac GTPases. Subsequent activation of phospholipase C (PLC) γ1 generates inositol triphosphate (IP_3), which binds to the IP_3 receptor (IP_3R), releasing Ca^{2+} from the endoplasmic reticulum (ER) and causing an increase in the intracellular Ca^{2+} concentration (Bustelo, 2001; Turner and Billadeau, 2002). Recently, a triple Vav knockout mouse was shown to have defects in antigen-stimulated Ca^{2+} signaling in B and T cells. However, rhythmic behaviors were not studied in these mice (Fujikawa et al., 2003).

Here we have found that VAV-1, the sole Vav-family protein in *C. elegans*, has a critical role in the three major rhythmic behaviors observed in the nematode. VAV-1 is expressed in the relevant tissues, and deletion of the *vav-1* gene results in a disruption of pharyngeal pumping and consequent early larval lethality. Lethality and pumping are rescued in transgenic *vav-1* deletion mutants by pharynx-specific expression of VAV-1. However, the transgenic *vav-1* mutants display severe defects in fertility and defecation secondary to disrupted gonadal and intestinal contractile rhythms, respectively. Our results provide new insights into the function of Vav proteins and demonstrate that VAV-1 has critical roles in regulating Ca^{2+} signaling and the generation of rhythmic behaviors.

Results

vav-1 Encodes a Putative Guanine Nucleotide Exchange Factor

The *C. elegans* genome contains a single putative open reading frame that encodes a polypeptide with greatest identity to members of the Vav family of GEFs. We isolated a full-length cDNA that is predicted to encode a 1007 amino acid protein, VAV-1 (Figure 1A). VAV-1 has

*Correspondence: maricq@biology.utah.edu
[5]These authors contributed equally to this work.

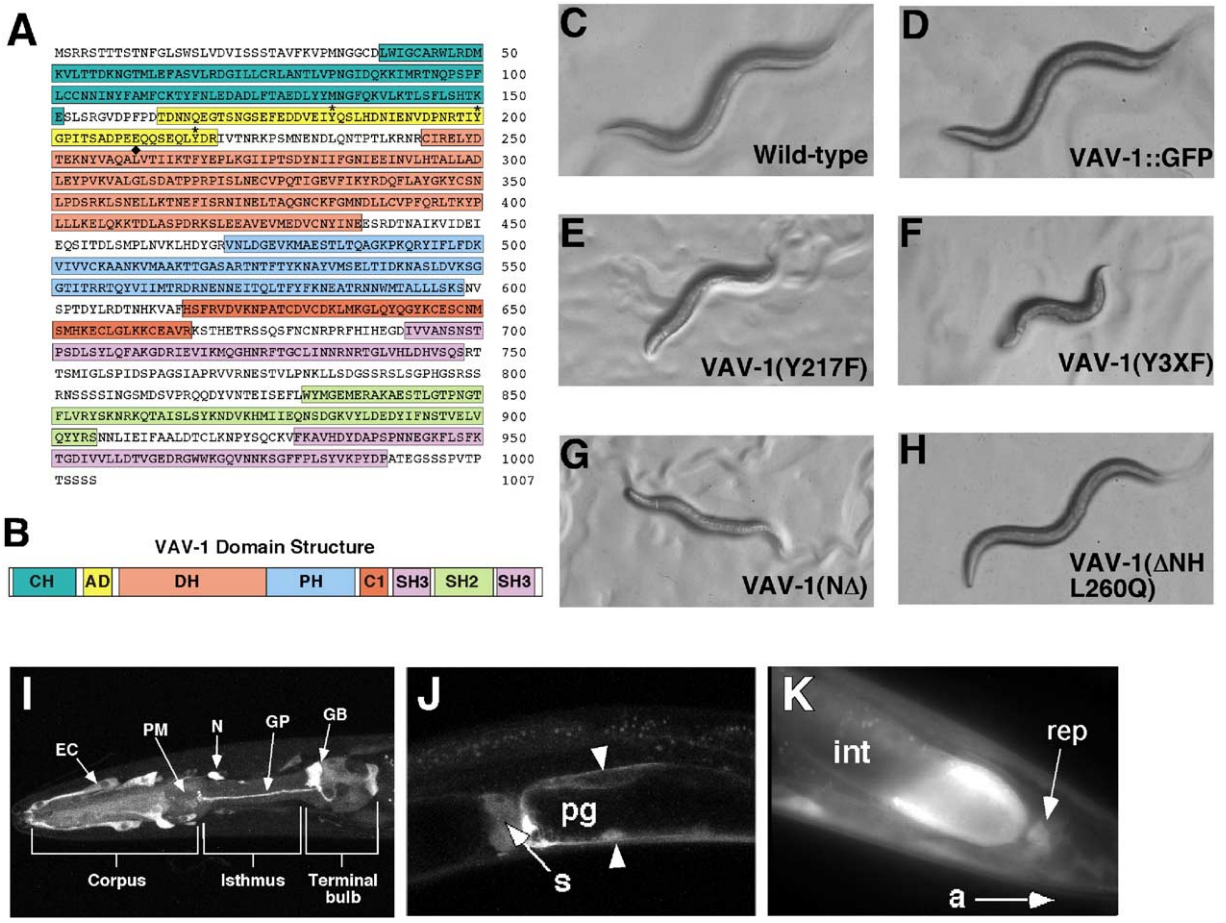

Figure 1. *C. elegans vav-1* Encodes a Vav-Family GEF that Is Expressed in Pharynx, Gonad, and Intestine

(A) Amino acid sequence of VAV-1. Conserved tyrosines that are characteristic of Vav proteins (Y183, Y200, and Y217) are indicated by asterisks. A conserved leucine in the DH domain that is essential for GEF function is indicated by a diamond.

(B) Domain structure of VAV-1. CH, calponin homology; AD, acidic; DH, Dbl homology; PH, plekstrin homology; C1, protein kinase C conserved region 1; SH2, Src homology 2; SH3, Src homology 3.

(C) Image of a wild-type animal.

(D–H) Transgenic worms expressing in muscle VAV-1::GFP (D); VAV-1::GFP(Y217F) (E); VAV-1(Y3XF) (F); VAV-1(NΔ) (G); VAV-1(NΔ);L260Q (H). For all animals, anterior is to the right.

(I) VAV-1::GFP expression in the pharynx. GFP is observed in the epidermal cells (EC), pharyngeal muscle (PM), neurons (N), and gland-cell body (GB) and process (GP).

(J) VAV-1::GFP expression in the spermatheca (s) and the sheath cells of the proximal gonad (pg). Arrowheads indicate sheath cells.

(K) VAV-1::GFP expression in the posterior intestine (int) and rectal epithelial cells (rep). The location of the anus is indicated (a).

all of the characteristic domains that are shared by other members of the vertebrate Vav protein family (Bustelo, 2001; Turner and Billadeau, 2002). These domains include the calponin homology (CH), acidic (AD), Dbl homology (DH), pleckstrin homology (PH), protein kinase C conserved region 1 (C1), Src homology 2 (SH2), and Src homology 3 (SH3) domains (Figure 1B). The DH domain is the signature feature of GEF proteins that catalyze the exchange of GDP for GTP on Rho family GTPases (Bustelo, 2001; Turner and Billadeau, 2002).

Characteristic of Vav proteins are several conserved tyrosine residues that are important for GEF activity. In murine Vav1, these include Tyr142, Tyr160, and Tyr174, which are rapidly phosphorylated by Syk- and Src-related tyrosine kinases in response to antigen stimulation of human B and T cells (Bustelo, 2001; Turner and Billadeau, 2002). Of these phosphorylation sites, Tyr174 has a key role in an autoinhibitory regulatory domain (Aghazadeh et al., 2000). Phosphorylation of Tyr174 promotes the displacement of this inhibitory region, leading to Vav1 GEF activation (Aghazadeh et al., 2000). The corresponding tyrosine residues are conserved in *C. elegans* VAV-1 (Tyr183, Tyr200, and Tyr217) (Figure 1A), suggesting that VAV-1 might be regulated by a similar mechanism.

To investigate the function of these conserved tyrosines, we used site-directed mutagenesis to generate Y217F and Y183F/Y200F/Y217F (Y3XF) mutant variants of VAV-1. We expressed these VAV-1 variants in transgenic worms using the body-wall-muscle-specific promoter, *myo-3.* We found that expression of the single

Y217F and the triple Y3XF mutant construct in the body-wall muscle led to a dominant hypercontracted and uncoordinated phenotype (Figures 1E and 1F). Additionally, we generated an N-terminal deletion of *vav-1*, known to result in oncogenic activity of mammalian Vav proteins (Bustelo, 2001; Turner and Billadeau, 2002), in which the CH and AD domains were removed. Expression of this deletion construct, *vav-1(NΔ)*, in the body-wall muscle using the *myo-3* promoter caused a phenotype identical to that observed in the Y217F and the Y3XF mutants (Figure 1G). To test whether this phenotype was due to unregulated GEF activity, we modified the *vav-1(NΔ)* construct by introducing the L260Q mutation (*vav-1(NΔ);L260Q*). The corresponding mutation in vertebrate Vav1 (L213Q) has been shown to substantially reduce in vivo GEF activity (Crespo et al., 1996, 1997). As predicted, transgenic worms that expressed *vav-1(NΔ);L260Q* had a wild-type phenotype, indicating that the dominant phenotype observed in transgenic worms that expressed *vav-1(NΔ)* was due to GEF activity (Figure 1H). We also used a biochemical assay to directly determine whether VAV-1 has GEF activity. We found that the purified DH/PH domain of VAV-1 was sufficient to promote GDP/GTP exchange on *C. elegans* Rho/Rac GTPases (Figure S1). These data demonstrate that *C. elegans* VAV-1 has GEF activity and that this activity, like that of the mammalian Vav family members, is regulated by tyrosine phosphorylation.

vav-1 Is Expressed in Tissues that Rhythmically Contract

To determine which cells express VAV-1, we used *vav-1* regulatory sequences to drive the expression of full length VAV-1 fused to the reporter molecule green fluorescent protein (GFP). In transgenic animals that express VAV-1::GFP, we observed strong GFP fluorescence in the pharynx, proximal gonad, spermatheca, intestine, and rectal epithelia (Figures 1I–1K). In the pharynx, VAV-1::GFP was observed in most cell types, including muscle cells, marginal cells, epithelial cells, neurons, and gland cells (Figure 1I). In the gonad, VAV-1::GFP was observed in the contractile sheath cells adjacent to the spermatheca (Figure 1J). The expression of VAV-1::GFP in the intestine was limited to the four most posterior cells (int8 and int9) and the three rectal epithelial cells (Figure 1K). Additionally, VAV-1::GFP expression was observed in the distal gonad, body-wall muscle, and vulval epithelia (data not shown).

vav-1 Mutants Cannot Feed and Die Early in Development

To determine the function of VAV-1, we generated a deletion mutation that removed approximately 2 kb of genomic sequence (Figure S2). Homozygous *vav-1(ak41)* mutants survive for many days but arrest at the first (L1) larval stage. Pharyngeal pumping in *vav-1* mutants was grossly abnormal—pharyngeal muscle contractions were either absent for long periods or asynchronous. We did not observe any obvious defects in pharyngeal morphology that might explain the disrupted pumping behavior. Likewise, the pharyngeal muscle displayed a normal radial arrangement of actin, and we observed no visible defects at the light-microscopic level in the organization of pharyngeal adherens junctions (Figure S3). Analysis of two other deletion alleles, *vav-1(ok425)* and *vav-1(tm402)*, revealed an L1 lethal phenotype identical to *vav-1(ak41)* mutants.

Pharyngeal function and lethality were rescued by expressing a VAV-1::GFP fusion protein under control of *vav-1* regulatory sequences (see below and Experimental Procedures). To test whether disruption of GEF activity accounted for the mutant phenotypes, we modified the rescuing VAV-1::GFP construct by introducing the L260Q mutation (Crespo et al., 1996, 1997). Transgenic *vav-1* mutants that expressed VAV-1(L260Q)::GFP at levels similar to rescuing VAV-1::GFP were defective in pharyngeal pumping, died as L1 larvae, and could not be distinguished from *vav-1* mutants (Figure S4). These results indicate that GEF activity is required for the normal function of *vav-1*.

vav-1 Is Required for Coordinated Pharyngeal Contraction

Analysis of the pharyngeal defect in *vav-1(ak41)* mutants using video microscopy and electrical recordings revealed asynchronous electrical activity of the pharyngeal musculature. During normal feeding, the radial muscles of the pharynx contract simultaneously to suck food into the opened lumen. A short while later, this process is reversed and the muscles relax, expelling fluid while retaining food (Albertson and Thomson, 1976). For this process to work efficiently, the muscle-cell contractions and relaxations must be synchronized (Avery and Thomas, 1997). Each pharyngeal pumping action is associated with a characteristic pattern of muscular electrical activity that can be recorded as an electropharyngeogram (EPG) (Avery et al., 1995).

Wild-type animals pump approximately 225 times per minute (Avery and Thomas, 1997). Each pump is associated with an excitatory depolarizing wave (E) followed by a plateau phase (P), often punctuated by brief negative spikes, and ending with an inhibitory hyperpolarizing wave (R) (Figure 2A). In contrast, EPGs recorded from *vav-1* mutants were highly disorganized (Figure 2B). Examination of mutant EPGs revealed occasional small-amplitude E waves that continued well into the plateau phase of each trace (Figure 2B). Accompanying video microscopy of wild-type (Figure 2D) and *vav-1* mutants (Figure 2E) revealed a lack of contractile activity in the corpus of the pharynx and unsynchronized contractile activity in the terminal bulb in mutants compared to wild-type. Although some muscle cells of the terminal bulb did visibly contract, these contractions were insufficient to open the pharyngeal lumen (Figure 2E, middle). Complete rescue of the EPG and pumping defects were observed in transgenic *vav-1* mutants that expressed VAV-1::GFP under the control of *vav-1* regulatory sequences (Figures 2C and 2F).

Since Vav proteins have been implicated in Ca^{2+} signaling in T and B cells (Bustelo, 2001; Turner and Billadeau, 2002), we measured pharyngeal Ca^{2+} transients in L1 larvae to determine whether the electrical defects were a result of abnormal Ca^{2+} signaling. As observed previously (Kerr et al., 2000), rhythmic increases in intracellular Ca^{2+} concentration could be detected in pharyngeal muscle cells of transgenic animals that ex-

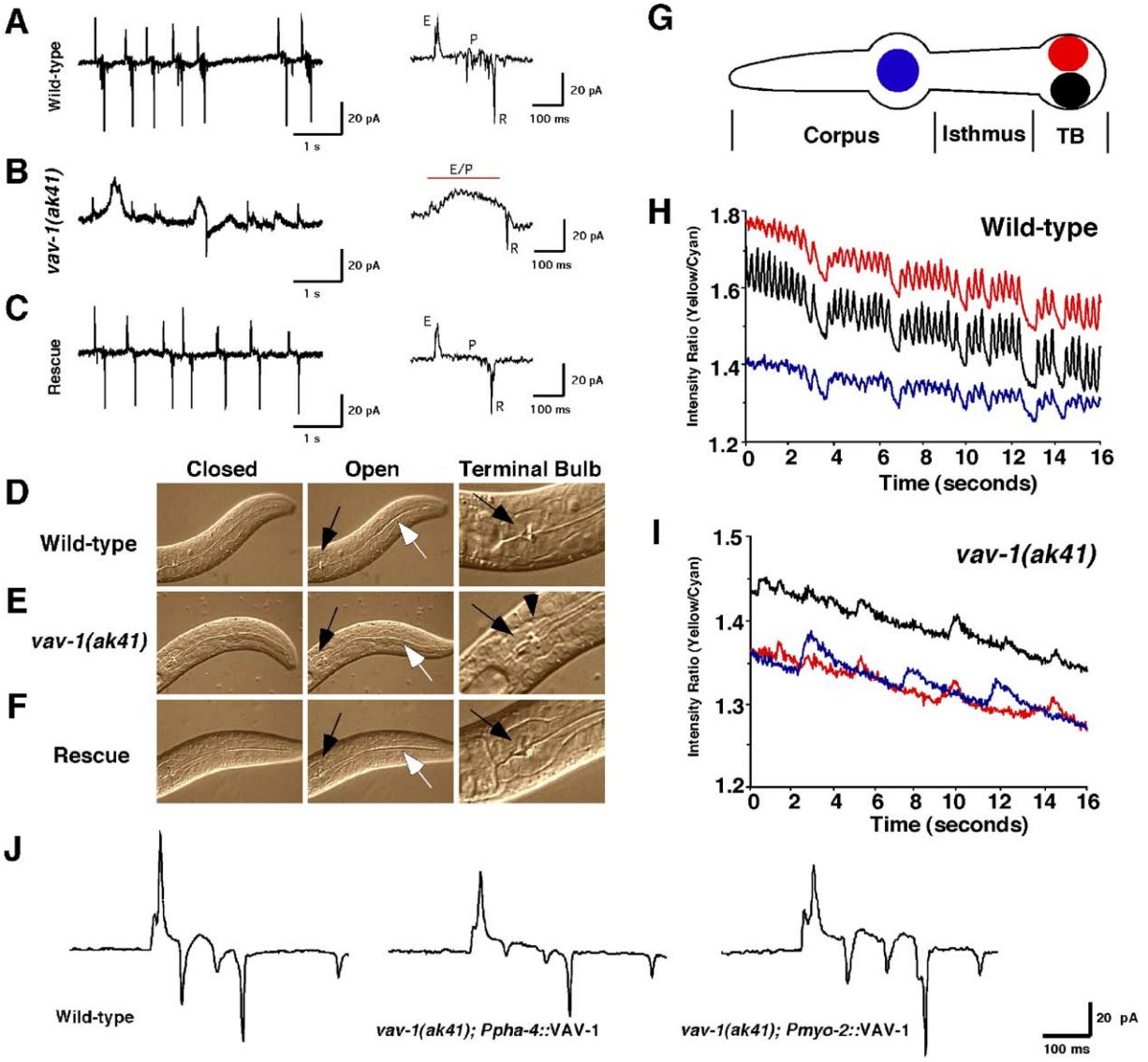

Figure 2. Pharyngeal Muscle Contractions Are Asynchronous in *vav-1* Mutants

(A–C) Representative EPG traces from L1 wild-type (A), *vav-1* (B), and a transgenic *vav-1* mutant expressing the VAV-1::GFP rescuing clone (C). Electrical activity corresponding to approximately seven pharyngeal contractions is shown on the left. A time-expanded inset of the EPG corresponding to a single pharyngeal contraction is shown on the right, with characteristic excitation (E), plateau (P), and relaxation (R) spikes.

(D–F) Video microscopy of pharyngeal muscle contractions in wild-type (D), *vav-1* (E), and a transgenic *vav-1* mutant expressing VAV-1::GFP (F). The black arrows identify the terminal bulb, and the white arrows indicate the open (D and F) or closed (E) pharyngeal lumen. The black arrowhead (E) points to a sole contracting pharyngeal muscle cell in *vav-1(ak41)*.

(G) Schematic representation of the pharynx of *C. elegans*. Filled circles within the pharynx indicate regions in which Ca^{2+} transients were measured. TB indicates terminal bulb of the pharynx.

(H and I) Ca^{2+} transients observed in a representative wild-type L1 pharynx (H) and *vav-1* mutant L1 pharynx (I). The traces in (H) and (I) correspond to the similarly colored regions of interest shown in (G). Although Ca^{2+} transients are observed in *vav-1* mutants, they are asynchronous and occur far less frequently.

(J) EPGs from representative wild-type and transgenic rescued *vav-1* animals expressing either *Pmyo-2*::VAV-1 or *Ppha-4*::VAV-1.

pressed cameleon, a ratiometric Ca^{2+} indicator (Miyawaki et al., 1997, 1999). The observed Ca^{2+} spikes always coincided with pharyngeal muscle contractions and pumping (Figure 2H). Interestingly, Ca^{2+} spikes were synchronous in the musculature of the corpus and the terminal bulb, indicating coordinated release of Ca^{2+} in these muscle groups of the pharynx. In contrast, Ca^{2+} spikes in *vav-1* mutants were infrequent and irregular (Figure 2I). Moreover, the synchronous Ca^{2+} spikes that occur within the corpus and the terminal bulb occur far less frequently in *vav-1* mutants (Figure 2I). Together, these results suggest that *vav-1* is required for the generation and synchronization of Ca^{2+} transients in the musculature of the pharynx.

To address whether the disrupted pharyngeal pumping observed in *vav-1* mutants was due to a defective pharynx or secondary to other defects, we used regulatory regions of the *pha-4* gene to drive the expression of VAV-1 in transgenic homozygous *vav-1* mutants. The *pha-4* promoter drives expression in almost all pharyngeal cells, including muscle cells, marginal cells, epithelial cells, gland cells, and most pharyngeal neurons (Horner et al., 1998; Kalb et al., 1998). In transgenic *vav-1* mutants that express *Ppha-4*::VAV-1, pumping and electrical activity are fully restored (Figure 2J), and the animals develop into viable adults. Because the pharyngeal Ca^{2+} imaging data suggest a specific requirement for VAV-1 in pharyngeal muscle, we attempted to rescue the *vav-1* mutant phenotype in transgenic animals by restricting VAV-1 expression to pharyngeal muscle using the *myo-2* promoter (Okkema et al., 1993). *vav-1* mutants that express *Pmyo-2*::VAV-1 have restored pharyngeal pumping, indicating that the pumping defects were due to altered pharyngeal muscle function (Figure 2J).

vav-1 Modulates Ovulation Rate via IP_3 and the Rho GTPases

We were able to characterize the function of VAV-1 in tissues other than the pharynx by studying transgenic *vav-1* mutants that expressed the *Ppha-4*::VAV-1 or *Pmyo-2*::VAV-1 transgene. Although these animals survived to adulthood and appeared to have normal locomotion, they had reduced fertility. The average brood size of transgenic hermaphrodites (*vav-1(ak41);Ppha-4*::VAV-1) was 44 ± 7.7 (n = 20), whereas wild-type hermaphrodites had 284 ± 4.9 progeny (n = 20) (Figure 3A). Furthermore, we found that *vav-1(ak41);Pmyo-2*::VAV-1 transgenic mutants had 21 ± 4.1 progeny (n = 40).

Vertebrate Vav1 is required for TCR-dependent intracellular Ca^{2+} signaling via activation of IP_3 receptors, which are intracellular Ca^{2+} release channels localized to the endoplasmic reticulum (Manetz et al., 2001; Reynolds et al., 2002). Previously, reduction-of-function mutations in the epidermal growth factor-like (EGF) gene, *lin-3*; the EGF-like receptor, *let-23* (Clandinin et al., 1998); and the inositol trisphosphate (IP_3) receptor, *itr-1* (Yin et al., 2004), were all found to disrupt ovulation, leading to a reduced brood size. A gain-of-function mutation (*gf*) in *itr-1* can partially suppress the reduced-brood-size defect in *let-23* and *lin-3* mutants (Clandinin et al., 1998). Moreover, loss-of-function mutations in the IP_3 kinase, *lfe-2*, and in a type I inositol polyphosphate 5-phosphatase, *ipp-5*, can also partially suppress the brood-size defect in *let-23* and *lin-3* mutants (Bui and Sternberg, 2002; Clandinin et al., 1998).

To investigate whether *vav-1* acts in an IP_3 signaling pathway, we generated double mutants or used RNA interference (RNAi) to knock down gene function. The brood size of *itr-1(gf);vav-1(ak41);Pmyo-2*::VAV-1 and *itr-1(gf);vav-1(ak41);Ppha-4*::VAV-1 double mutants was significantly larger than *vav-1(ak41);Pmyo-2*::VAV-1 and *vav-1(ak41);Ppha-4*::VAV-1 mutants alone, respectively (Figure 3A). Additionally, *lfe-2(RNAi)* or *ipp-5(RNAi)* to *vav-1(ak41);Pmyo-2*::VAV-1 mutants significantly suppressed the brood defect (Figure 3A). Further support for the hypothesis that *vav-1* functions to regulate IP_3 comes from double mutants containing a reduction-of-function mutation in the IP_3 receptor, *itr-1(rf)*, and *vav-1(ak41);Ppha-4::vav-1* mutants. These mutants were almost completely sterile, displaying phenotypic enhancement over either single mutation (Figure 3A). To investigate the possibility of *vav-1* acting in the EGF signaling pathway during ovulation, we made double mutants with *vav-1;Ppha-4*::VAV-1 and a gain-of-function mutation in the EGF receptor, *let-23(gf)*. Unlike *itr-1(gf)*, *let-23(gf)* did not significantly improve the brood-size defect observed in *vav-1(ak41);Ppha-4*::VAV-1 mutants (Figure 3A). This suggests that the *let-23*/EGFR acts upstream of *vav-1* to promote ovulation.

Since *vav-1* is also expressed in the vulval epithelia, it is possible that an egg-laying defect may contribute to the smaller brood size observed in *vav-1(ak41);Ppha-4*::VAV-1 mutants. However, mutants that are defective in egg laying typically are bloated with retained eggs. In contrast, *vav-1* mutants did not appear bloated by visual inspection. Eggs that are retained due to a laying defect will have progressed further in development. Therefore, a microscopic examination of recently laid eggs provides a more sensitive assay for defects in egg laying. Eggs from wild-type and *vav-1(ak41);Ppha-4*::VAV-1 mutants were indistinguishable, indicating that *vav-1* mutants do not have an egg-laying defect (Figure 3B). In contrast, eggs laid by *egl-19(n582)* mutants (defective in contraction of the vulval muscles) (Lee et al., 1997; Trent et al., 1983) were at a much later developmental stage.

Low brood size can be caused by other factors, such as impaired sperm production or mobility or defective ovulation. VAV-1 is expressed in the gonadal-sheath cells and spermatheca, suggesting that VAV-1 may also be required for ovulation or sperm function. However, mating wild-type males with *vav-1* mutant hermaphrodites did not restore the brood size to normal levels (Figure 3C), indicating that the reduced fertility of *vav-1* mutants was more likely due to an ovulation defect. To test this hypothesis, we video-recorded sheath-cell contractions and ovulations from immobilized worms. We found that the basal sheath-cell contraction rate was slower in mutants. In wild-type animals, the average basal contraction rate is approximately 8 contractions/min, whereas in *vav-1;Ppha-4*::VAV-1 and *vav-1;Pmyo-2*::VAV-1 mutants the contraction rate is approximately 5 and 2 contractions/min, respectively (Figure 3D).

We next examined the cellular events associated with ovulation. In wild-type animals, oocytes align on the proximal-distal axis of the gonad and undergo a series of changes during ovulation that occur in an assembly-line manner (McCarter et al., 1999). These consist of oocyte maturation, which includes nuclear-envelope breakdown and cortical rearrangement; dilation of the spermatheca; and sheath-cell contractions, which pull the dilated spermatheca over the mature oocyte, allowing entry into the spermatheca and fertilization (Figure 4A). In both *vav-1(ak41);Ppha-4*::VAV-1 and *vav-1(ak41);Pmyo-2*::VAV-1 mutants, the oocytes developed normally until they reached the spermatheca. However, at this point, several defects were observed, such as ovulation of immature oocytes (Figure 4B), premature spermatheca constriction (Figure 4C), and overexten-

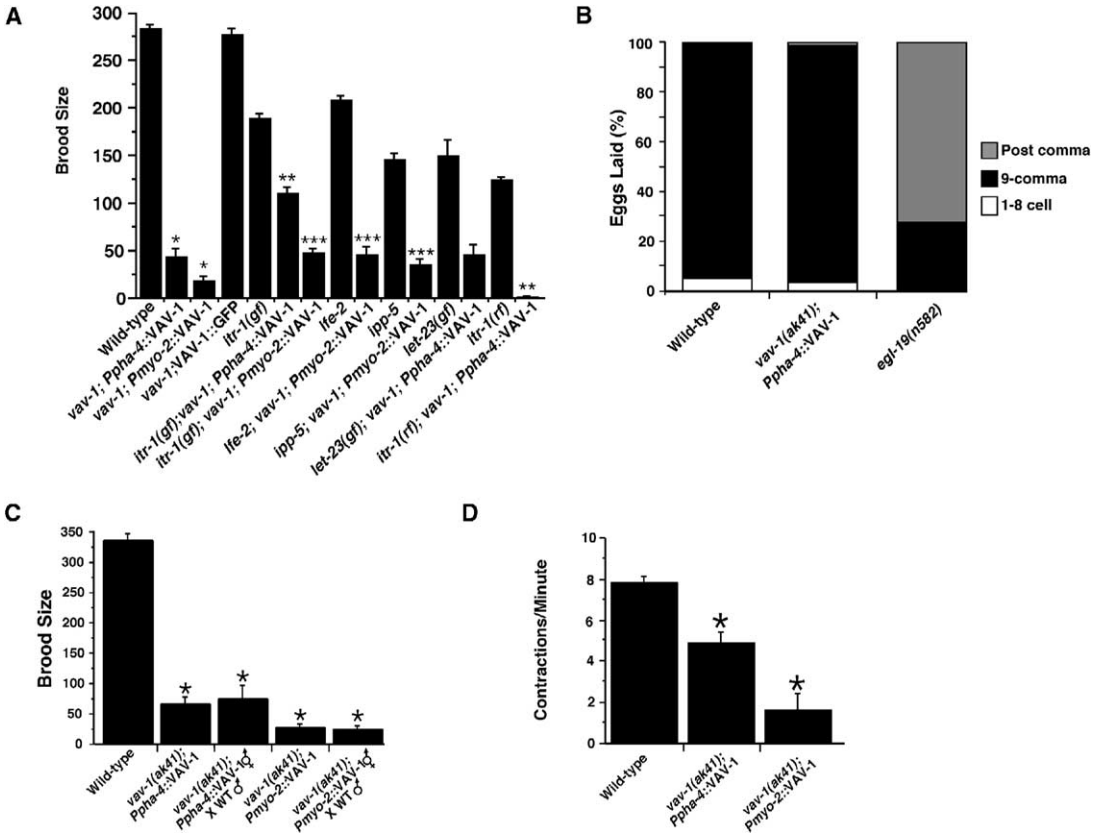

Figure 3. *vav-1* Mutants Have Reduced Fertility and Irregular Gonadal-Sheath-Cell Contractions

(A) Brood size. Statistically different from wild-type (*p < 0.0001), *vav-1;Ppha-4*::VAV-1 (**p < 0.0001), or *vav-1;Pmyo-2*::VAV-1 (***p < 0.0001).

(B) Egg-laying behavior. The stage of freshly laid eggs was scored and classified as 1–8 cell stage, 9 cell–comma stage, and postcomma. More than 100 eggs were scored for each genotype.

(C) Brood size following mating with wild-type (wt) males. Statistically different from wild-type (*p < 0.0001).

(D) Basal sheath-cell contraction rate. *vav-1;Ppha-4*::VAV-1 mutants are statistically different from both wild-type (*p < 0.0001) and *vav-1; Pmyo-2*::VAV-1 mutants (*p < 0.0005). Error bars indicate standard error of the mean (SEM).

sion of the spermatheca past the proximal oocyte. (Figure 4D). These defects were associated with constriction and damage of the oocyte. Additionally, we occasionally observed that the oocytes did not enter the spermatheca in *vav-1(ak41);Pmyo-2*::VAV-1 mutants and arrested with an endomitotic phenotype (Figure 4E). In sum, our data indicate that *vav-1* is required for the normal coordination of sheath-cell contractions, spermathecal dilation, and oocyte maturation and likely acts through the IP_3R.

Since we found that VAV-1 acts as a Rho/Rac-family guanine nucleotide exchange factor (Figure S1), we investigated whether disrupting any of the Rho/Rac GTPases of *C. elegans* causes defects in ovulation. *C. elegans* contains three genes encoding Rac GTPases, *ced-10*, *mig-2*, and *rac-2* (Chen et al., 1993a; Lundquist et al., 2001); one Rho GTPase, *rho-1*; and one Cdc42 GTPase, *cdc-42* (Chen et al., 1993b; Chen and Lim, 1994). Analysis of RNAi knockdown of candidate Rho/Rac GTPase-encoding genes or analysis of known mutants revealed that only *rho-1(RNAi)* had a phenotype similar to *vav-1(ak41);Pmyo-2*::VAV-1 mutants (Figure 4F). Double-mutant analysis of *cdc-42(RNAi);mig-2* and *cdc-42(RNAi);ced-10* revealed severe migration defects of the gonadal distal-tip cells, resulting in abnormal gonad development. *ced-10;mig-2* mutants also had gonadal migration defects as well as oocyte development defects. These findings prevented analysis of ovulation in these double mutants. These data indicate that *vav-1* is involved in regulating ovulation by modulating IP_3 signaling and that this signaling pathway may involve the small GTPase *rho-1*.

vav-1 Function Is Required for a Normal Defecation Cycle

Defecation in *C. elegans* is composed of three sequential motor steps: posterior body-wall-muscle contraction (pBoc), anterior body-wall-muscle contraction (aBoc), and enteric-muscle contraction (Emc) leading to expulsion (Avery and Thomas, 1997). This motor program is repeated approximately every 45–50 s. In *vav-1;Ppha-4*::VAV-1 mutants, the three sequential motor steps occurred normally, i.e., once initiated, the timing and order of the three steps was normal. However, the cycle period (defined by the interval between successive pBocs) was irregular, and the mean cycle time was lengthened to approximately 85 s (Figures 5A and 5C). Because the *pha-4* promoter is weakly expressed in

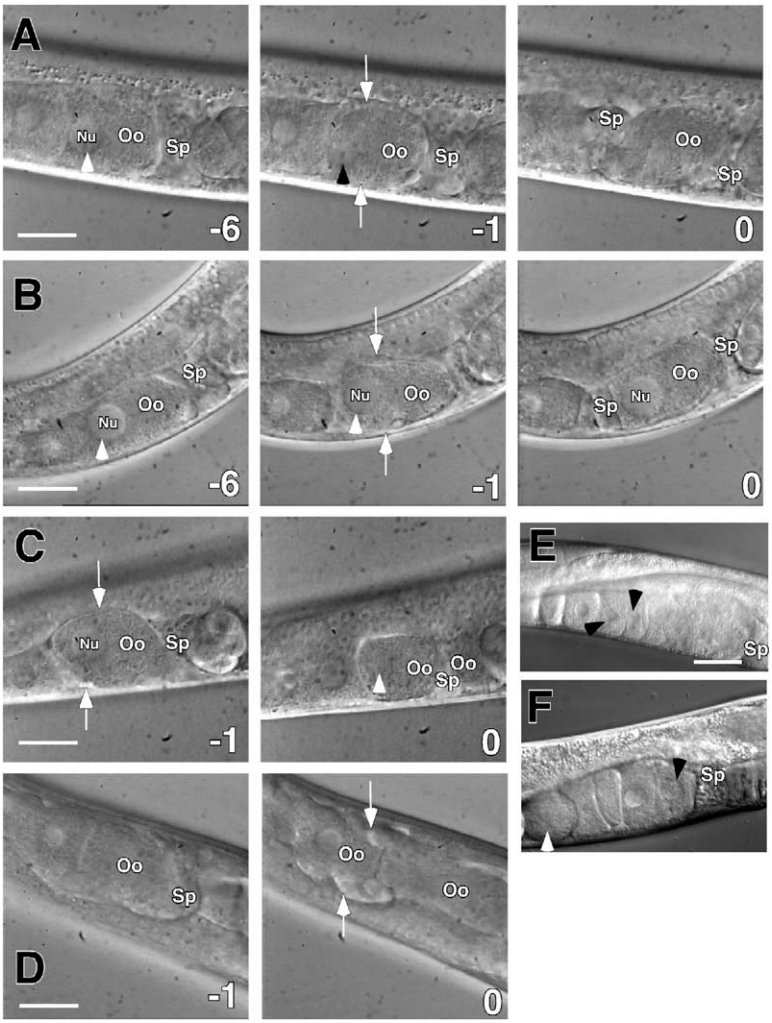

Figure 4. Ovulation Is Defective in *vav-1* Mutants

(A–D) Ovulation events in wild-type (A) and transgenic *vav-1;Ppha-4*::VAV-1 animals (B–D). Numbers indicate the time (min) prior to ovulation, with ovulation occurring at time 0. Oo, oocyte; Sp, spermatheca; Nu, nucleus. (A and B) The nucleus is clearly discernable (arrowhead) in the left panel. (A) Coincident with nuclear-envelope breakdown (black arrowhead; middle panel), the oocyte enters the spermatheca. (B) Nuclear envelope breakdown does not occur in the *vav-1* mutant (arrowhead; middle panel). The arrows indicate the spermatheca engulfing the oocyte. The right panels show an oocyte completely engulfed by the spermatheca. Note the presence of a discernable nucleus in the mutant (B) compared to wild-type (A). (C) An oocyte in a *vav-1* mutant that is severed in half by the spermatheca (right). In this example, the nuclear envelope has broken down (arrowhead). (D) The spermatheca of a *vav-1* mutant overextends and pinches (arrows) the second oocyte.

(E) In transgenic *vav-1;Pmyo-2*::VAV-1 mutants, many oocytes fail to enter the spermatheca, resulting in the accumulation of endomitotic oocytes (arrowheads).

(F) In a *rho-1(RNAi)* worm, oocytes fail to enter the spermatheca and become endomitotic (black arrowhead); a more distal oocyte undergoes maturation precociously (white arrowhead). In all pictures, the vulva is to the right. Scale bar = 25 μm.

intestinal cells (Kalb et al., 1998), we also examined defecation in *vav-1(ak41);Pmyo-2*::VAV-1 mutants. While these animals still defecate, the average cycle duration was approximately 195 s, the cycle was highly variable and irregular (Figures 5A–5C), and frequently the expulsion step was skipped.

We used mosaic analysis to identify the cells in which VAV-1 function is required for the periodicity of defecation (Figure 6). To do this, we characterized defecation in transgenic *vav-1* mutants expressing two linked transgenes: the *vav-1* rescuing genomic clone and a *Psur-5::NLS::GFP* clone that is expressed in the nuclei of all somatic cells and is a well-established tool for mosaic analysis (Yochem et al., 1998). We found that, in all cases, young adult mosaic animals lacking the transgenes in the E lineage, which gives rise to the intestine, were defecation defective (Figure 6). Furthermore, in cases where the transgenes were present in the E lineage, the defecation cycle was normal.

vav-1 Controls the Duration of the Defecation Cycle via IP_3 and the Rho/Rac GTPases

The IP_3 receptor has also been implicated in the control of the defecation cycle. Loss-of-function mutations in *itr-1* result in the slowing or absence of the pBoc-pBoc defecation cycle (Dal Santo et al., 1999). To investigate whether the gain-of-function *itr-1(gf)* mutation could suppress the impaired defecation in *vav-1* mutants, we examined the defecation cycle in *itr-1(gf);vav-1(ak41); Pmyo-2*::VAV-1 mutants. Consistently, the defecation-cycle rhythm was improved in *itr-1(gf);vav-1(ak41); Pmyo-2*::VAV-1 double mutants compared to *vav-1(ak41);Pmyo-2*::VAV-1 single mutants. (Figure 5A). We also found partial suppression of the defecation-cycle-rhythm defect in *vav-1(ak41);Pmyo-2*::VAV-1 mutants treated with *lfe-2(RNAi)* (Figure 5A). In contrast, we did not observe suppression in mutants treated with *ipp-5(RNAi)* (Figure 5A). Additionally, we examined double mutants containing a reduction-of-function allele of *itr-1* and *vav-1(ak41);Ppha-4*::VAV-1 and found that the defecation cycle was significantly extended in the double mutant as compared to the single mutants (Figure 5A). These data suggest that *vav-1* functions via IP_3 signaling to regulate the defecation cycle.

Does VAV-1 signal through the *C. elegans* Rho/Rac GTPases to control the timing of the defecation cycle? To determine whether these genes are involved, we examined the defecation cycle in known mutants or used RNAi knockdown of specific Rho/Rac GTPases. RNAi knockdown of *cdc-42*, *ced-10*, *mig-2*, *rac-2*, and *rho-1*

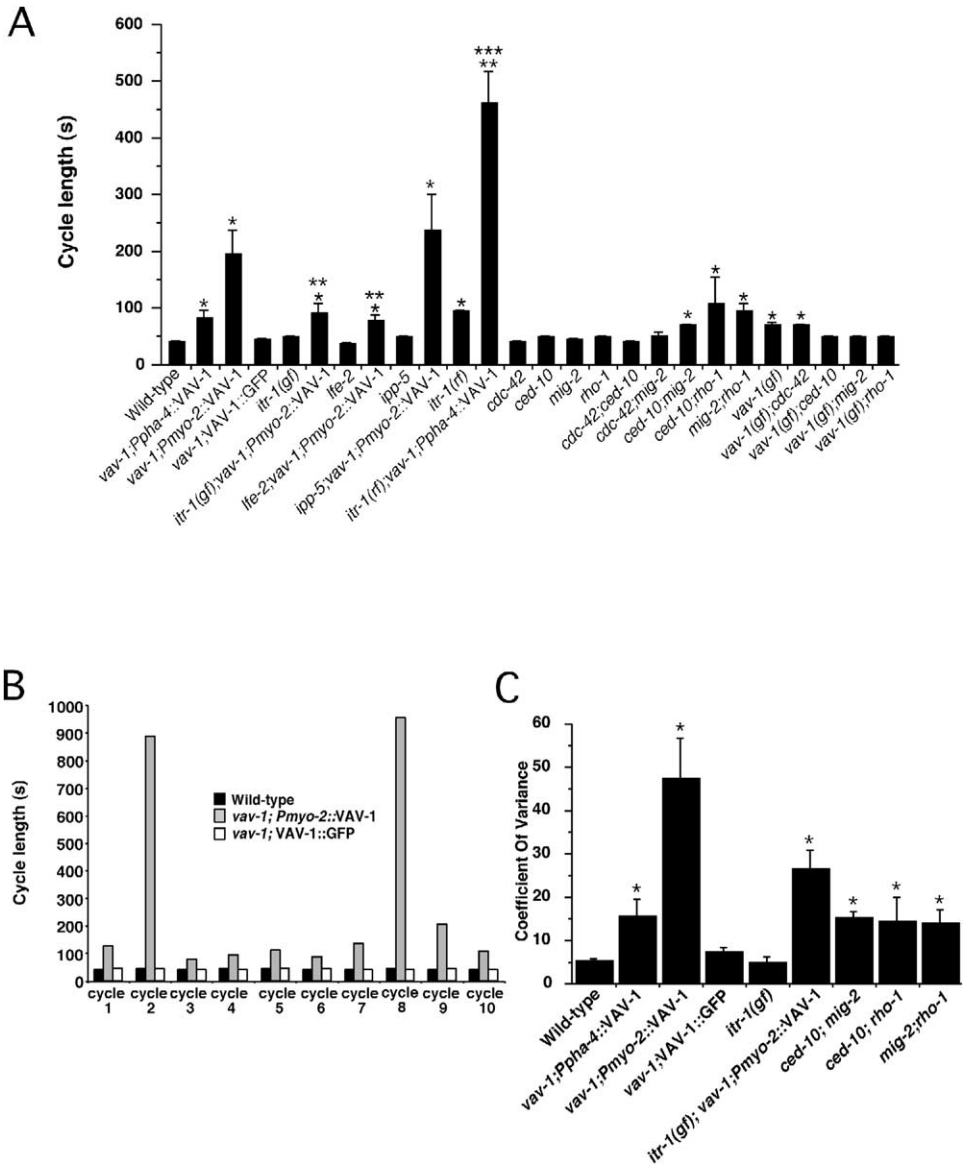

Figure 5. The Timing of the Defecation Cycle Is Altered in *vav-1* Mutants

(A) Average time interval between consecutive pBocs. Statistically different from wild-type (*p $\leq$ 0.0001), *vav-1;Pmyo-2*::VAV-1 (**p $\leq$ 0.02), *vav-1;Ppha-4*::VAV-1, or *itr-1(rf)*(***p $\leq$ 0.0001).

(B) The duration of ten defecation cycles in representative wild-type, *vav-1;Pmyo-2*::VAV-1, and *vav-1* rescued animals.

(C) Coefficient of variance. Statistically different from wild-type (*p $\leq$ 0.02). Error bars indicate SEM.

individually did not reveal any significant defects in defecation timing (Figure 5A and data not shown). Additionally, analysis of *ced-10* and *mig-2* single mutants did not reveal any significant defecation timing defects (Figure 5A). Given that there are five genes encoding Rho/Rac GTPases in *C. elegans*, it is possible that there is genetic redundancy. Consistent with this, we found that RNAi knockdown of *rho-1* in the mutant background of *ced-10* or *mig-2* caused an extended and arrhythmic defecation cycle (Figures 5A and 5C). Moreover, we found that *ced-10;mig-2* double mutants had significantly lengthened and arrhythmic defecation cycles (Figures 5A and 5C). We could not extend this analysis because *rho-1* RNAi knockdown in the *ced-10;mig-2* double mutant was larval lethal. In contrast, we observed no defecation defects in *cdc-42(RNAi); mig-2* and *cdc-42(RNAi);ced-10* mutants. These data demonstrate that *ced-10*, *mig-2*, and *rho-1* have a redundant function in controlling the periodicity of the defecation cycle.

To further dissect the role of *vav-1* and the Rho/Rac GTPases, we engineered a constitutively active GEF mutation (Y3XF) (see above) in VAV-1 that was expressed solely in the intestine by the *ges-1* promoter, *Pges-1::vav-1(gf)*. Expression of *Pges-1::vav-1(gf)* in wild-type animals resulted in abnormal defecation-

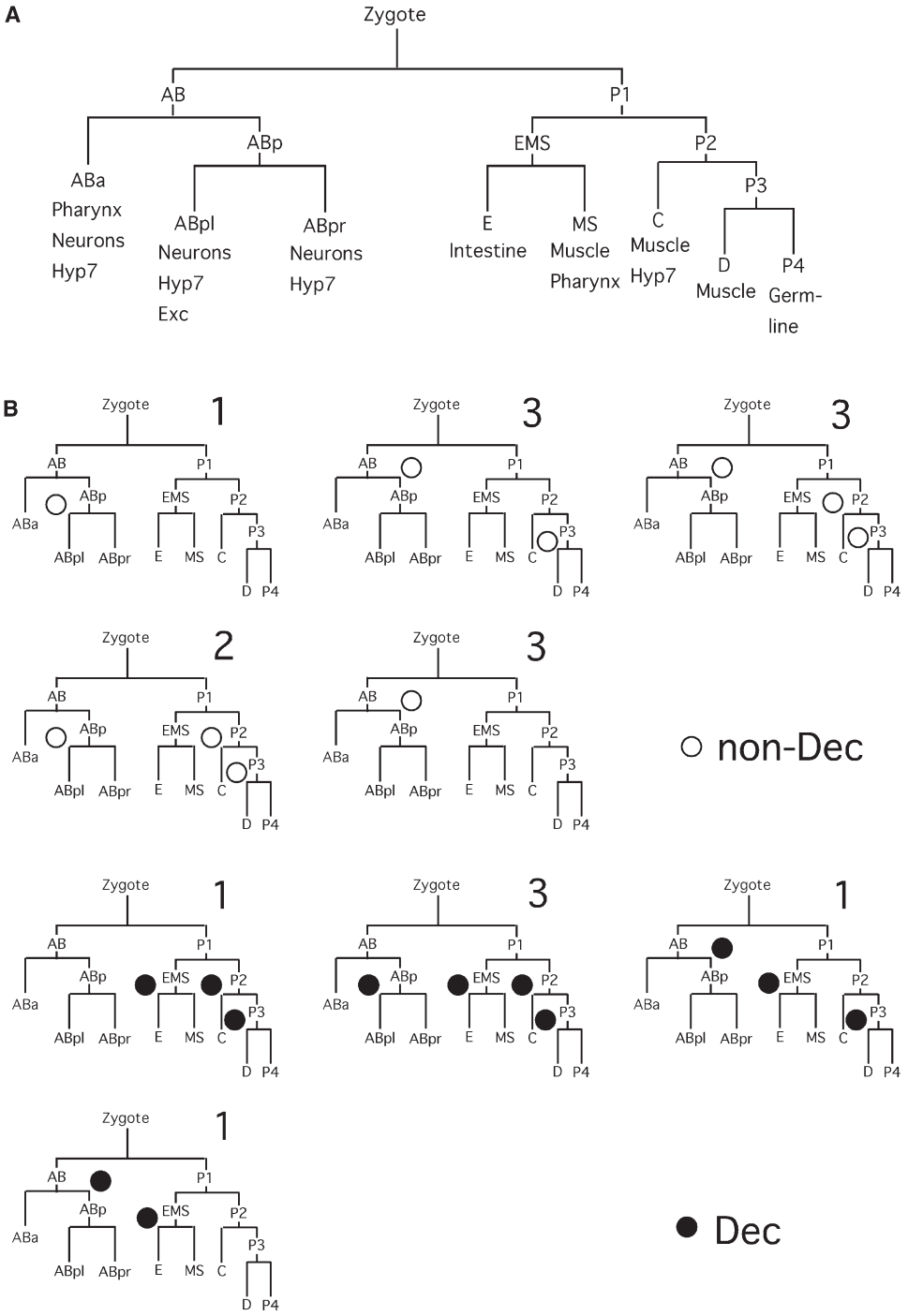

Figure 6. VAV-1 Expression in the Intestine Restores the Defecation Cycle in *vav-1* Mutants

(A) Cell lineage of *C. elegans*, indicating the tissue that arises from each lineage. Exc is the excretory cell, and Hyp7 denotes the cells that make up the epidermis.

(B) Mosaic animals are represented by a cell lineage. The number above the lineage indicates the number of animals in each class. The open circle represents where in the embryonic lineage the extrachromosomal array was lost in non-defecation-defective (non-Dec) mosaic animals. The closed circle represents where in the embryonic lineage the array was lost in defecation-defective (Dec) mosaic animals.

cycle timing. The defecation cycle of these animals was arrhythmic and extended compared to wild-type animals that did not express the *Pges-1::vav-1(gf)* transgene (Figure 5A). To determine whether the Rho/Rac GTPases act downstream of *vav-1*, we carried out RNAi knockdown experiments of the Rho/Rac GTPases in animals expressing the *Pges-1::vav-1(gf)* transgene. We found that RNAi knockdown of *ced-10*, *mig-2*, and

rho-1 could suppress the defecation timing defect observed in *Pges-1::vav-1(gf)*-expressing animals (Figure 5A). In contrast, *cdc-42(RNAi)* did not significantly suppress the defecation timing defects of *Pges-1::vav-1(gf)*-expressing animals (Figure 5A). These data indicate that *ced-10*, *mig-2*, and *rho-1* act downstream of *vav-1* to regulate defecation-cycle timing.

VAV-1 may function in a signaling pathway to activate phosphatidylinositol 4-phosphate 5 kinase (PIP5K) to generate phosphatidylinositol(4,5)biphosphate (PIP2), the substrate for IP_3 production. To test this hypothesis, we knocked down the function of *ppk-1*/PIP5K by RNAi and found an almost complete absence of the defecation cycle (no pBoc observed in > 600 s of observation), indicating a critical role for PIP5K in the control of defecation. To test whether VAV-1 functions upstream of PIP5K, we also knocked-down *ppk-1*/PIP5K in transgenic worms that expressed *vav-1(gf).* The phenotype of the worms following RNAi was similar to *ppk-1* alone (no pBoc observed in > 600 s of observation), indicating that *ppk-1*/PIP5K acts downstream of *vav-1*. These results indicate that IP_3 production is dependent on the activation of VAV-1

Intracellular Ca^{2+} Oscillations Are Abnormal in *vav-1* Mutants

Our genetic evidence indicates that *vav-1* is required for IP_3 generation. Thus, in *vav-1* mutants, the release of Ca^{2+} from intracellular stores may be impaired, leading to impaired rhythmic contractility. Since Ca^{2+} signaling in the pharynx was abnormal in *vav-1* mutants, we also investigated Ca^{2+} signaling in the intestines. To analyze intracellular Ca^{2+} oscillations, we loaded isolated intestines with the indicator Fluo-4 and imaged fluorescence intensity (see Experimental Procedures). In wild-type animals, Ca^{2+} oscillations were observed at very regular intervals, similar to the timing of the defecation cycle, and were highly reproducible (Figures 7A, 7D, and 7E). In contrast, *vav-1;Pmyo-2*::VAV-1 mutants had an arrhythmic and lengthened Ca^{2+} oscillation frequency similar to the defective defecation behavior observed in these animals (Figures 7B, 7D, and 7E). Additionally, we found that the lengthened Ca^{2+} oscillation frequency observed in *vav-1;Pmyo-2*::VAV-1 mutants was suppressed by a gain-of-function mutation in *itr-1*; however, the frequency of Ca^{2+} signaling remains arrhythmic (Figures 7D and 7E). Consistent with the Rho/Rac GTPases acting downstream of VAV-1, *ced-10;mig-2* mutants showed a phenotype similar to *vav-1; Pmyo-2*::VAV-1. The double mutant had arrhythmic and lengthened defecation cycles (Figures 7C–7E). These results suggest that VAV-1 regulates Ca^{2+} oscillations via Rho GTPases within the intestines to control the rhythmic behavior of the defecation cycle.

Discussion

We have found that *vav-1* is required for three different rhythmic behaviors: the synchronous pumping of the pharynx, the coordinated contractions of sheath cells and dilation of the spermatheca, and the periodicity of the defecation cycle. We have also shown that, in the intestines, VAV-1 function is dependent on members of the Rho/Rac family of GTPases and IP_3 signaling. These data suggest that VAV-1 is part of a signaling pathway used by a variety of tissues to control the release of intracellular Ca^{2+} and generate rhythmic activity. Consistent with this model, we observed abnormal Ca^{2+} transients in pharyngeal muscle and the intestines of *vav-1* mutants and Rho/Rac double mutants.

VAV-1 Is Required for Synchronous Contraction of the Pharynx

In *vav-1* mutants, pharyngeal contraction is weak and asynchronous, leading to ineffectual pharyngeal pumping and consequent early larval death. We have shown that VAV-1 expression in pharyngeal muscle is sufficient to rescue the pharyngeal pumping defects of *vav-1* mutants. How then might VAV-1 affect pharyngeal muscle function? One could imagine that *vav-1* mutants have defects in muscle depolarization, excitation-contraction coupling, myosin-dependent force generation, or gap-junction-mediated communication between pharyngeal muscle cells. The asynchrony of terminal-bulb-muscle cell contraction and the abnormal, long-duration EPG traces from *vav-1* mutants suggest that the cellular defect may originate from disrupted electrical conduction, defective Ca^{2+} release from intracellular stores, or the diffusion of Ca^{2+} between neighboring muscle cells.

We found abnormal Ca^{2+} transients in the pharyngeal musculature of *vav-1* mutants. Interestingly, a null mutation in the gene encoding sarcoendoplasmic reticulum Ca^{2+} transport ATPase (*sca-1*), which is required for restoring Ca^{2+} stores, results in an L1 lethal phenotype that is very reminiscent of *vav-1* mutants (Zwaal et al., 2001). Furthermore, mutations in Ca^{2+} channels that are expressed in the pharynx result in abnormal pharyngeal contraction. These include the *egl-19* L type voltage-gated Ca^{2+} channel α1 subunit (Lee et al., 1997), the *unc-68* ryanodine receptor (Maryon et al., 1996; Sakube et al., 1993), and the *itr-1* IP_3 receptor (Walker et al., 2002). In addition, the pharyngeal muscle cells are connected to one another by gap junctions formed by innexins (Phelan and Starich, 2001; Starich et al., 2001), and mutations in these proteins disrupt coordinated contraction (Li et al., 2003; Starich et al., 1996). Therefore, VAV-1 may also regulate the activity of the innexin proteins, thus preventing Ca^{2+} diffusion to other muscle cells. However, altered Ca^{2+} levels only partly explain the abnormal EPG, which measures ion flux across the cell membrane. The altered EPG suggests that the activity of plasma-membrane ion channels is altered, either directly via VAV-1 signaling pathways or indirectly via the action of Ca^{2+} ions.

Sheath-Cell Contractions and Ovulation Are Disrupted in *vav-1* Mutants

The synchronized contractions of the sheath cells and dilation of the spermatheca are dependent on EGF signaling (Bui and Sternberg, 2002; Clandinin et al., 1998; McCarter et al., 1999; Yin et al., 2004). Reduction-of-function mutations in either the EGF-like protein, *lin-3*, or the EGF-like receptor, *let-23*, cause sterility because the spermatheca does not dilate. Similar to *lin-3* and *let-23* mutants, *vav-1* mutants have a greatly reduced brood size, and this defect is suppressed by a gain-of-function mutation in the IP_3 receptor, *itr-1*, and func-

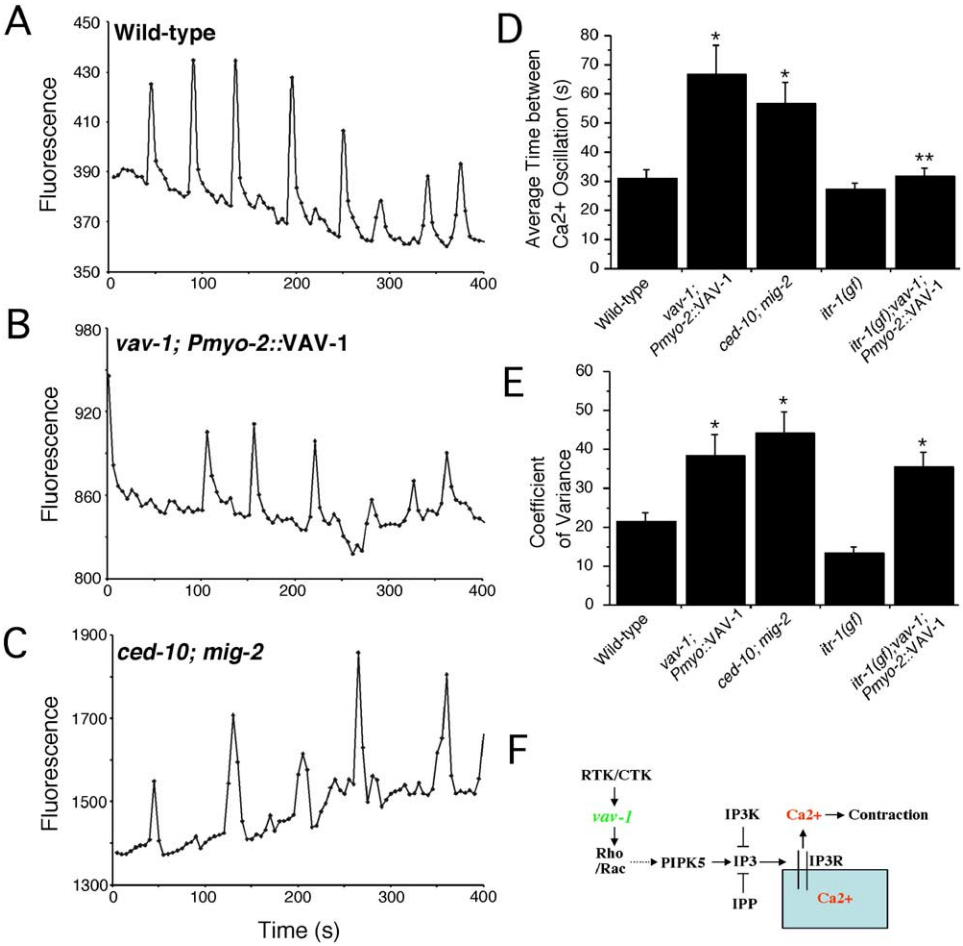

Figure 7. Intestinal Ca^{2+} Transients Are Altered in *vav-1* Mutants

(A–C) Intestinal Ca^{2+} transients observed in a representative wild-type (A), *vav-1* mutant (B), and *ced-10; mig-2* double mutant (C).

(D) Quantification of time between consecutive Ca^{2+} oscillations. Statistically different from wild-type (*$p \leq 0.005$) and *vav-1(ak41);Pmyo-2*::VAV-1 (**$p \leq 0.0001$).

(E) Coefficient of variance. Statistically different from wild-type (*$p \leq 0.01$).

(F) Model of *vav-1* signaling during fertilization and defecation timing. Abbreviations are as indicated in the text except the following: RTK, receptor tyrosine kinase; CTK, cytoplasmic tyrosine kinase; IPP, type I inositol 5-phosphatase. Error bars indicate SEM.

tional knockdown of the IP_3 kinase, *lfe-2*, and a type I inositol 5-phosphatase, *ipp-5*. Moreover, we have found a phenotypic enhancement when a weak loss-of-function mutation of the IP_3R, *itr-1(rf)*, is introduced into the *vav-1;Ppha-4*::VAV-1 background (weak *vav-1* background). In addition, a gain-of-function mutation in *let-23*/EGFR could not bypass the brood-size defect observed in *vav-1* mutants. These data suggest that *vav-1* acts upstream of IP_3 signaling and downstream of the EGFR. Consistent with the idea of *vav-1* acting downstream of EGF signaling, mammalian Vav family members have also been implicated in EGF signaling (Bustelo and Barbacid, 1992; Margolis et al., 1992; Movilla and Bustelo, 1999; Pandey et al., 2000), and, in *Drosophila*, DroVav has been found to be highly phosphorylated after EGF receptor activation (Hornstein et al., 2003).

How might *vav-1* function in the *C. elegans* EGF/IP_3 signaling pathway? As suggested by the mammalian and *Drosophila* studies, LIN-3/EGF stimulation may lead to rapid phosphorylation and activation of VAV-1. In mammalian cells, phosphorylated VAV-1 activates PLCγ to generate IP_3 (Manetz et al., 2001; Reynolds et al., 2002). Consistent with PLCγ having a role in ovulation, RNAi inactivation of the *C. elegans* PLCγ (*plc-3*) results in a severe defect in ovulation (Yin et al., 2004). Alternatively, VAV-1 may activate PIP5K, which generates PIP2, the substrate of PLCγ. Consistent with this model, studies of signaling in B lymphocytes have suggested that Vav1 activates PIP5K (O'Rourke et al., 1998). *C. elegans* has three genes encoding PIP5K-like proteins, *ppk-1*, *ppk-2*, and *ppk-3*, and a *C. elegans* genome-wide RNAi screen has revealed a sterility defect in *ppk-1(RNAi)*-treated animals (Kamath et al., 2003; Simmer et al., 2003).

The Defecation Cycle in *vav-1* Mutants Is Irregular

The defecation cycle in *C. elegans* is highly regular, so much so that it has been termed a cellular clock (Dal Santo et al., 1999; Iwasaki and Thomas, 1997). In con-

trast, the cycle in *vav-1* mutants is arrhythmic and no longer clock-like, suggesting that VAV-1 either is part of a clock or is a critical modulator of a complex rhythm. In mammalian cells, Vav is known to be regulated by external signals acting through membrane receptors (Bustelo, 2001; Turner and Billadeau, 2002). By analogy, we expect that receptor-mediated signaling regulates rhythmic activity via activation of VAV-1. In support of this hypothesis, the defecation cycle is dependent on the presence of food (Iwasaki and Thomas, 1997), indicating the possible involvement of other signaling pathways. In addition, cycle duration approximately doubles when the concentration of food is lowered (Liu and Thomas, 1994) and decreases in duration with temperature shifts from 20°C to 25°C (Branicky et al., 2001), again suggesting that sensory input regulates the defecation rhythm.

Previous experiments demonstrated that IP_3 receptor function in the intestine was required for the defecation cycle and that a Ca^{2+} spike, which occurred approximately every 50 s in the intestine, was absent in *itr-1* IP_3 receptor null mutants or slowed in the hypomorphic mutant (Dal Santo et al., 1999). We found that a gain-of-function mutation in *itr-1*, which leads to a 2-fold increase in IP_3 affinity (Walker et al., 2002), was capable of partially suppressing the defecation defects observed in *vav-1* mutants. Furthermore, we found that *lfe-2(RNAi)* could also partially suppress the defecation defect observed in *vav-1* mutants. In contrast, *ipp-5(RNAi)* did not significantly suppress the defecation defect. However, *ipp-5* is only expressed in the spermatheca and the proximal gonad (Bui and Sternberg, 2002), whereas *itr-1* and *lfe-2* are both reported to be expressed in the intestine as well as the gonad/spermatheca (Baylis et al., 1999; Dal Santo et al., 1999; Clandinin et al., 1998). As was observed for gonad function, we found a synthetic enhancement of the duration of the defecation cycle when a weak loss-of-function mutation of the IP_3R, *itr-1*, was introduced into the *vav-1;Ppha-4::vav-1* background, providing further evidence that *vav-1* functions via IP_3 to regulate the rhythm of the defecation cycle. Additionally, we found that RNAi of Rho/Rac GTPases causes abnormal defecation cycles in wild-type worms and could partially suppress the defecation defects caused by the overexpression of a *vav-1(gf)* transgene. We also found that RNAi of *ppk-1*/PIP5K causes a defective defecation cycle. Consistent with *C. elegans* Rac and Rho proteins acting to modulate IP_3 levels, both mammalian Rac1 and RhoA have been implicated in the activation of PIP5K (O'Rourke et al., 1998; Saci and Carpenter, 2005). Together, our data suggest a model where VAV-1 functions in the intestine via the Rho/Rac GTPases to modulate IP_3 signaling and the rhythm of the defecation cycle (Figure 7F).

In summary, our data indicate that VAV-1 has an evolutionarily conserved role in Ca^{2+} signaling and modulates three major rhythmic behaviors found in *C. elegans*. These rhythms are considered nonneurogenic in that they do not appear to be directly driven by nervous-system input and thus may be more analogous to the intrinsic rhythms found in tissues such as the vertebrate heart, which are modulated by external signals. In the absence of VAV-1, Ca^{2+} signaling and pumping, ovulation, and defecation behaviors are still present, but the cycles are longer and arrhythmic. Because VAV-1 is required for three different rhythmic behaviors in *C. elegans*, VAV-1 may act as a global regulator of biological rhythms through its modulation of Ca^{2+} oscillations. Since biological rhythms are a critical feature of all organisms, it is possible that VAV-1-like proteins have similar roles in other biological systems.

Experimental Procedures

General Methods and Strains

Strains were maintained using standard procedures. Wild-type refers to the Bristol N2 strain, and the mutant alleles are listed in the Supplemental Experimental Procedures. All experiments, unless otherwise noted, were carried out at 24°C. Brood sizes were established by placing single L4 hermaphrodites of each genotype on individual plates with the *E. coli* strain OP50. Animals were transferred to fresh plates containing OP50 every 12 hr for 4 days. The resulting F1 progeny were counted shortly after the transfer of hermaphrodites. For each genotype, a minimum of 20 animals were scored. Defecation-cycle length in young adult animals was carried out as described (Dal Santo et al., 1999). Mosaic analysis was carried out as described (Yochem and Herman, 2003). RNAi was carried out as described (Kamath et al., 2003; Simmer et al., 2003; Timmons et al., 2001), except for the analysis of *rho-1* and *cdc-42*. RNAi to *cdc-42* and *rho-1* was conducted on L1 larvae, and young adults were examined. Statistical analysis was carried out by ANOVA and unpaired t tests using StatView. Coefficient of variance was calculated by standard deviation/mean × 100.

Ca^{2+} Imaging

Pharyngeal cameleon Ca^{2+} imaging was carried out on a Zeiss Axioplan 2 microscope equipped with a Roper Cascade 512B CCD camera, a Dual View beam splitter (Optical Instruments), and a Lambda DG4 light source (Sutter). For pharyngeal recordings, L1 larvae were immobilized in M9 containing 1 mM levamisole and 10 mM serotonin. Images were collected at ~20 Hz (5 ms exposure time) using a Zeiss 100× 1.4 N.A. Plan-Apochromat. For Fluo-4 (Molecular Probes) loading, animals were dissected by decapitation, and the intestine was allowed to partially exit the body cavity. Intestines were loaded with 1–5 μM Fluo-4 for 10 min and then thoroughly washed with buffer (described in Supplemental Experimental Procedures). Images were collected every 1–5 s (100–200 ms exposure time) using a Zeiss 40× 1.3 N.A. Plan Neofluar objective lens. All fluorescence images were acquired and analyzed using MetaFluor 6.2r2 (Universal Imaging).

Supplemental Data

Supplemental Data include Supplemental Experimental Procedures, Supplemental References, and four figures and can be found with this article online at http://www.cell.com/cgi/content/full/123/1/119/DC1/.

Acknowledgments

We thank E. Jorgensen, L. Lim, S. Mango, J. McGhee, T. Pawson and H. Qadota for reagents; P. Sternberg, B. Schafer, the *Caenorhabditis* Genetics Center, and the *C. elegans* Gene Knockout Consortium for strains; A. Fire for the plasmid vector kit; R. Barstead for a cDNA library; R. Steven and T. Kubiseski for technical advice; G. Prestwich and M. Horvath for use of their equipment; P. Brockie for technical assistance; and members of the Maricq lab for valuable discussions and critical reading of the manuscript. This work was supported by the Huntsman Cancer Foundation (M.C.B.), the American Cancer Society (A.V.M.), the NSF (Career Award 9876262 to A.V.M.), and the NIH (NS35812 to A.V.M. and HL60591 to M.C.B.). K.R.N. was supported by the NRSA F32 GM066579-02 and T32 CA93247. R.T.F. was supported by the American Heart Association.

Received: August 27, 2004
Revised: June 4, 2005
Accepted: August 5, 2005
Published: October 6, 2005

References

Aghazadeh, B., Lowry, W.E., Huang, X.Y., and Rosen, M.K. (2000). Structural basis for relief of autoinhibition of the Dbl homology domain of proto-oncogene Vav by tyrosine phosphorylation. Cell *102*, 625–633.

Albertson, D.G., and Thomson, J.N. (1976). The pharynx of Caenorhabditis elegans. Philos. Trans. R. Soc. Lond. B Biol. Sci. *275*, 299–325.

Avery, L., and Thomas, J.H. (1997). Feeding and defecation. In C. elegans II, D.L. Riddle, T. Blumenthal, B.J. Meyer, and J.R. Preiss, eds. (Cold Spring Harbor, NY: Cold Spring Harbor Laboratory Press), pp. 679–716.

Avery, L., Raizen, D., and Lockery, S. (1995). Electrophysiological methods. Methods Cell Biol. *48*, 251–269.

Baylis, H.A., Furuichi, T., Yoshikawa, F., Mikoshiba, K., and Sattelle, D.B. (1999). Inositol *1*, 4, 5 trisphosphate receptors are strongly expressed in the nervous system, pharynx, intestine, gonad and excretory cell of Caenorhabditis elegans and are encoded by a single gene (itr-1). J. Mol. Biol. *294*, 467–476.

Branicky, R., Shibata, Y., Feng, J., and Hekimi, S. (2001). Phenotypic and suppressor analysis of defecation in clk-1 mutants reveals that reaction to changes in temperature is an active process in Caenorhabditis elegans. Genetics *159*, 997–1006.

Bui, Y.K., and Sternberg, P.W. (2002). Caenorhabditis elegans inositol 5-phosphatase homolog negatively regulates inositol 1,4,5-triphosphate signaling in ovulation. Mol. Biol. Cell *13*, 1641–1651.

Bustelo, X.R. (2001). Vav proteins, adaptors and cell signaling. Oncogene *20*, 6372–6381.

Bustelo, X.R., and Barbacid, M. (1992). Tyrosine phosphorylation of the vav proto-oncogene product in activated B cells. Science *256*, 1196–1199.

Chen, W., and Lim, L. (1994). The Caenorhabditis elegans small GTP-binding protein RhoA is enriched in the nerve ring and sensory neurons during larval development. J. Biol. Chem. *269*, 32394–32404.

Chen, W., Lim, H., and Lim, L. (1993a). A new member of the ras superfamily, the rac1 homologue from Caenorhabditis elegans. Cloning and sequence analysis of cDNA, pattern of developmental expression, and biochemical characterization of the protein. J. Biol. Chem. *268*, 320–324.

Chen, W., Lim, H., and Lim, L. (1993b). The CDC42 homologue from Caenorhabditis elegans. Complementation of a yeast mutation. J. Biol. Chem. *268*, 13280–13285.

Clandinin, T.R., DeModena, J.A., and Sternberg, P.W. (1998). Inositol trisphosphate mediates a RAS-independent response to LET-23 receptor tyrosine kinase activation in C. elegans. Cell *92*, 523–533.

Crespo, P., Bustelo, X.R., Aaronson, D.S., Coso, O.A., Lopez-Barahona, M., Barbacid, M., and Gutkind, J.S. (1996). Rac-1 dependent stimulation of the JNK/SAPK signaling pathway by Vav. Oncogene *13*, 455–460.

Crespo, P., Schuebel, K.E., Ostrom, A.A., Gutkind, J.S., and Bustelo, X.R. (1997). Phosphotyrosine-dependent activation of Rac-1 GDP/GTP exchange by the vav proto-oncogene product. Nature *385*, 169–172.

Dal Santo, P., Logan, M.A., Chisholm, A.D., and Jorgensen, E.M. (1999). The inositol trisphosphate receptor regulates a 50-second behavioral rhythm in C. elegans. Cell *98*, 757–767.

Fujikawa, K., Miletic, A.V., Alt, F.W., Faccio, R., Brown, T., Hoog, J., Fredericks, J., Nishi, S., Mildiner, S., Moores, S.L., et al. (2003). Vav1/2/3-null mice define an essential role for Vav family proteins in lymphocyte development and activation but a differential requirement in MAPK signaling in T and B cells. J. Exp. Med. *198*, 1595–1608.

Horner, M.A., Quintin, S., Domeier, M.E., Kimble, J., Labouesse, M., and Mango, S.E. (1998). pha-4, an HNF-3 homolog, specifies pharyngeal organ identity in Caenorhabditis elegans. Genes Dev. *12*, 1947–1952.

Hornstein, I., Mortin, M.A., and Katzav, S. (2003). DroVav, the Drosophila melanogaster homologue of the mammalian Vav proteins, serves as a signal transducer protein in the Rac and DER pathways. Oncogene *22*, 6774–6784.

Iwasaki, K., and Thomas, J.H. (1997). Genetics in rhythm. Trends Genet. *13*, 111–115.

Kalb, J.M., Lau, K.K., Goszczynski, B., Fukushige, T., Moons, D., Okkema, P.G., and McGhee, J.D. (1998). pha-4 is Ce-fkh-1, a fork head/HNF-3alpha,beta,gamma homolog that functions in organogenesis of the C. elegans pharynx. Development *125*, 2171–2180.

Kamath, R.S., Fraser, A.G., Dong, Y., Poulin, G., Durbin, R., Gotta, M., Kanapin, A., Le Bot, N., Moreno, S., Sohrmann, M., et al. (2003). Systematic functional analysis of the Caenorhabditis elegans genome using RNAi. Nature *421*, 231–237.

Kerr, R., Lev-Ram, V., Baird, G., Vincent, P., Tsien, R.Y., and Schafer, W.R. (2000). Optical imaging of calcium transients in neurons and pharyngeal muscle of C. elegans. Neuron *26*, 583–594.

Lee, R.Y., Lobel, L., Hengartner, M., Horvitz, H.R., and Avery, L. (1997). Mutations in the alpha1 subunit of an L-type voltage-activated Ca2+ channel cause myotonia in Caenorhabditis elegans. EMBO J. *16*, 6066–6076.

Li, S., Dent, J.A., and Roy, R. (2003). Regulation of intermuscular electrical coupling by the Caenorhabditis elegans innexin inx-6. Mol. Biol. Cell *14*, 2630–2644.

Liu, D.W., and Thomas, J.H. (1994). Regulation of a periodic motor program in C. elegans. J. Neurosci. *14*, 1953–1962.

Lundquist, E.A., Reddien, P.W., Hartwieg, E., Horvitz, H.R., and Bargmann, C.I. (2001). Three C. elegans Rac proteins and several alternative Rac regulators control axon guidance, cell migration and apoptotic cell phagocytosis. Development *128*, 4475–4488.

Manetz, T.S., Gonzalez-Espinosa, C., Arudchandran, R., Xirasagar, S., Tybulewicz, V., and Rivera, J. (2001). Vav1 regulates phospholipase cgamma activation and calcium responses in mast cells. Mol. Cell. Biol. *21*, 3763–3774.

Margolis, B., Hu, P., Katzav, S., Li, W., Oliver, J.M., Ullrich, A., Weiss, A., and Schlessinger, J. (1992). Tyrosine phosphorylation of vav proto-oncogene product containing SH2 domain and transcription factor motifs. Nature *356*, 71–74.

Maryon, E.B., Coronado, R., and Anderson, P. (1996). unc-68 encodes a ryanodine receptor involved in regulating C. elegans body-wall muscle contraction. J. Cell Biol. *134*, 885–893.

McCarter, J., Bartlett, B., Dang, T., and Schedl, T. (1997). Soma-germ cell interactions in Caenorhabditis elegans: multiple events of hermaphrodite germline development require the somatic sheath and spermathecal lineages. Dev. Biol. *181*, 121–143.

McCarter, J., Bartlett, B., Dang, T., and Schedl, T. (1999). On the control of oocyte meiotic maturation and ovulation in Caenorhabditis elegans. Dev. Biol. *205*, 111–128.

Miyawaki, A., Llopis, J., Heim, R., McCaffery, J.M., Adams, J.A., Ikura, M., and Tsien, R.Y. (1997). Fluorescent indicators for Ca2+ based on green fluorescent proteins and calmodulin. Nature *388*, 882–887.

Miyawaki, A., Griesbeck, O., Heim, R., and Tsien, R.Y. (1999). Dynamic and quantitative Ca2+ measurements using improved cameleons. Proc. Natl. Acad. Sci. USA *96*, 2135–2140.

Movilla, N., and Bustelo, X.R. (1999). Biological and regulatory properties of Vav-3, a new member of the Vav family of oncoproteins. Mol. Cell. Biol. *19*, 7870–7885.

Okkema, P.G., Harrison, S.W., Plunger, V., Aryana, A., and Fire, A. (1993). Sequence requirements for myosin gene expression and regulation in Caenorhabditis elegans. Genetics *135*, 385–404.

O'Rourke, L.M., Tooze, R., Turner, M., Sandoval, D.M., Carter, R.H., Tybulewicz, V.L., and Fearon, D.T. (1998). CD19 as a membrane-anchored adaptor protein of B lymphocytes: costimulation of lipid and protein kinases by recruitment of Vav. Immunity *8*, 635–645.

Pandey, A., Podtelejnikov, A.V., Blagoev, B., Bustelo, X.R., Mann, M., and Lodish, H.F. (2000). Analysis of receptor signaling pathways by mass spectrometry: identification of vav-2 as a substrate of the epidermal and platelet-derived growth factor receptors. Proc. Natl. Acad. Sci. USA *97*, 179–184.

Phelan, P., and Starich, T.A. (2001). Innexins get into the gap. Bioessays *23*, 388–396.

Reynolds, L.F., Smyth, L.A., Norton, T., Freshney, N., Downward, J., Kioussis, D., and Tybulewicz, V.L. (2002). Vav1 transduces T cell receptor signals to the activation of phospholipase C-gamma1 via phosphoinositide 3-kinase-dependent and -independent pathways. J. Exp. Med. *195*, 1103–1114.

Saci, A., and Carpenter, C.L. (2005). RhoA GTPase regulates B cell receptor signaling. Mol. Cell *17*, 205–214.

Sakube, Y., Ando, H., and Kagawa, H. (1993). Cloning and mapping of a ryanodine receptor homolog gene of Caenorhabditis elegans. Ann. N Y Acad. Sci. *707*, 540–545.

Schuebel, K.E., Bustelo, X.R., Nielsen, D.A., Song, B.J., Barbacid, M., Goldman, D., and Lee, I.J. (1996). Isolation and characterization of murine vav2, a member of the vav family of proto-oncogenes. Oncogene *13*, 363–371.

Simmer, F., Moorman, C., Van Der Linden, A.M., Kuijk, E., Van Den Berghe, P.V., Kamath, R., Fraser, A.G., Ahringer, J., and Plasterk, R.H. (2003). Genome-wide RNAi of C. elegans using the hypersensitive rrf-3 strain reveals novel gene functions. PLoS Biol. *1*, e12. 10.1371/journal.pbio.0000012

Starich, T., Sheehan, M., Jadrich, J., and Shaw, J. (2001). Innexins in C. elegans. Cell Commun. Adhes. *8*, 311–314.

Starich, T.A., Lee, R.Y., Panzarella, C., Avery, L., and Shaw, J.E. (1996). eat-5 and unc-7 represent a multigene family in Caenorhabditis elegans involved in cell-cell coupling. J. Cell Biol. *134*, 537–548.

Thomas, J.H. (1990). Genetic analysis of defecation in Caenorhabditis elegans. Genetics *124*, 855–872.

Timmons, L., Court, D.L., and Fire, A. (2001). Ingestion of bacterially expressed dsRNAs can produce specific and potent genetic interference in Caenorhabditis elegans. Gene *263*, 103–112.

Trent, C., Tsuing, N., and Horvitz, H.R. (1983). Egg-laying defective mutants of the nematode Caenorhabditis elegans. Genetics *104*, 619–647.

Turner, M., and Billadeau, D.D. (2002). VAV proteins as signal integrators for multi-subunit immune-recognition receptors. Nat. Rev. Immunol. *2*, 476–486.

Walker, D.S., Gower, N.J., Ly, S., Bradley, G.L., and Baylis, H.A. (2002). Regulated disruption of inositol 1,4,5-trisphosphate signaling in Caenorhabditis elegans reveals new functions in feeding and embryogenesis. Mol. Biol. Cell *13*, 1329–1337.

Yin, X., Gower, N.J., Baylis, H.A., and Strange, K. (2004). Inositol 1,4,5-trisphosphate signaling regulates rhythmic contractile activity of myoepithelial sheath cells in Caenorhabditis elegans. Mol. Biol. Cell *15*, 3938–3949.

Yochem, J., and Herman, R.K. (2003). Investigating C. elegans development through mosaic analysis. Development *130*, 4761–4768.

Yochem, J., Gu, T., and Han, M. (1998). A new marker for mosaic analysis in Caenorhabditis elegans indicates a fusion between hyp6 and hyp7, two major components of the hypodermis. Genetics *149*, 1323–1334.

Zwaal, R.R., Van Baelen, K., Groenen, J.T., van Geel, A., Rottiers, V., Kaletta, T., Dode, L., Raeymaekers, L., Wuytack, F., and Bogaert, T. (2001). The sarco-endoplasmic reticulum Ca2+ ATPase is required for development and muscle function in Caenorhabditis elegans. J. Biol. Chem. *276*, 43557–43563.